Biochemistry

 Volume 41, Number 27 July 9, 2002

Accelerated Publications

Absolute Measurement of Phosphorylation Levels in a Biological Membrane Using Atomic Force Microscopy: The Creation of Phosphorylation Maps†

Je-Wen Liou, Xavier Mulet, and David R. Klug*

Molecular Dynamics Group, Biological and Biophysical Chemistry Section, Department of Chemistry, Imperial College of Science Technology and Medicine, Exhibition Road, London SW7 2AZ, U.K.

Received April 15, 2002; Revised Manuscript Received May 22, 2002

ABSTRACT: We show that it is possible to produce phosphorylation difference maps of biological membranes under conditions which reflect those in vivo and in which proteins remain functional. We also demonstrate that absolute levels of phosphorylation are retrieved through the application of an appropriate calibration method. Finally we show that the kinetics of phosphorylation/dephosphorylation can also be monitored. These methods are demonstrated on photosynthetic membranes from higher plants, for which protein phosphorylation is the dominant regulatory mechanism. We show directly that the most recent estimates of the phosphorylation levels in this system are reasonably accurate. Phosphorylation difference maps show that the distribution of phosphates is not even, with significantly higher levels at the membrane margins and patches of high phosphate density next to patches of low charge density.

Protein phosphorylation is one of the most widely used posttranslational modifications of proteins in living cells. Reversible phosphorylations of membrane proteins and lipids are responsible for modulating and controlling a range of processes as diverse as enzyme control, membrane trafficking, and protein turnover. In higher plant photosynthesis, it is believed that most of the phosphorylatable proteins are those associated with photosystem II (mostly on light-harvesting complex II, LHC II).[1] The phosphorylation of proteins controls the stacking and unstacking of photosynthetic membranes. This membrane stacking in turn affects the extent of intermixing and level of communication between photosystems I and II (PS I and PS II) and the cytochrome b_6f complex (*1*). One major effect of these changes is to modify the partitioning of excitation energy between PS I and PS II and possibly the balance of cyclic and linear electron transport. It has been shown that 20−23% of grana membranes (PS II membranes) unstack after phosphorylation (*1*, *2*). It is also suggested that the phosphorylation of PS II membrane proteins can stabilize the PS II D1, D2 heterodimer structure and consequently increase the tolerance of the PS II reaction center to light inhibition (*3*). Several kinases responsible for phosphorylation of the thylakoid membranes are light-activated and are tentatively

† This work was financially supported by the Biotechnology and Biological Science Research Council, United Kingdom.

* Correspondence should be addressed to this author (e-mail: d.klug@ic.ac.uk).

[1] Abbreviations: AFM, atomic force microscope; ATP, adenosine triphosphate; e_c, electrolyte concentration; ΔZ, electrostatic force height contribution in AFM experiments; DLVO, Derjaguin, Landau, Verwey, Overbeek; α-DM, *n*-dodecyl-α-D-maltoside; DOPC, 1,2-dioleoyl-*sn*-glycero-3-phosphocholine; ϵ_e, dielectric constant; ϵ_0, permittivity of the free space; F_{DLVO}, DLVO force; F_{el}, electrostatic interaction; F_{vdw}, van der Waals interaction; H_a, Hamaker constant; λ_D, Debye length; LHC II, light-harvesting complex II; P_i, inorganic phosphate group; PIP2, L-α-phosphatidylinositol-4,5-diphosphate; PS I, photosystem I; PS II, photosystem II; R, AFM tip radius; σ_s, charge density of sample surface; σ_t, charge density of AFM tip surface.

10.1021/bi025962s CCC: $22.00
Published on Web 06/12/2002

identified as membrane proteins (*4*−*10*). Although reversible phosphorylation of the proteins associated with photosystem II is a dominant control mechanism, the levels of phosphorylation are not known. Evidence has accumulated regarding the number of phosphorylation sites and their locations, but there has been no way of monitoring the absolute amount of charge placed on the membrane surface by the action of light-activated kinases. This makes it difficult to understand the mechanism of membrane stacking/unstacking and impossible to quantify the relationship between kinase activity and photosynthetic function. To better understand this relationship, we have developed a method for measuring absolute levels of charge on a membrane surface using an atomic force microscope, under conditions in which the proteins remain functional. We expect this approach to be helpful in studying other membrane systems in which reversible phosphorylation plays a role. In fact, the calibration method that we have developed allows the levels of surface charges to be measured accurately under a range of aqueous conditions, something which may be of utility in many areas of membrane research.

Since the invention of the atomic force microscope (AFM) in 1986 (*11*), the AFM has shown itself to be a powerful tool for imaging the topography of surfaces. As the force that AFM applies to the sample surfaces can be as little as 10^{-11} N, it can also be used to detect small forces from surface charges (*12*−*15*). In this paper, an atomic force microscope was used to detect the change of electrostatic interaction resulting from the light-driven phosphorylation (*5*) of the spinach PS II enriched membrane.

MATERIALS AND METHODS

Atomic Force Microscopy. A commercial AFM (Explorer, Thermomicroscope) equipped with a liquid 100 μm scanner was used. The 200 μm long cantilevers with oxide-sharpened Si_3N_4 tips used in the experiments were purchased from Digital Instruments. The spring constant of these cantilevers was 0.06 nN/nm. AFM samples were prepared by dropping the diluted membrane sample onto fresh cleaved mica. After an adsorption time of 40−60 min, the samples were gently washed with the imaging buffer to remove the membranes which were not attached. The AFM samples were then imaged in buffer. The forces applied on the samples were 0.6 nN as measured by the AFM controller and software. The scan rate was 2−4 lines/s.

PS II Enriched Membranes. PS II enriched thylakoid membranes (BBYs) were prepared from dark-adapted market spinach leaves as described by D. A. Berthold, G. T. Babcock, and C. F. Yocum, (*16*). The PS II membrane was then destacked using the method described by (*17*) with some modifications. BBYs at a chlorophyll concentration of 1.4 mg/mL in 20 mM Bis-Tris buffer, pH 6.5, and 5 mM $MgCl_2$ were treated with *n*-dodecyl-α,D-maltoside (α-DM, final concentration 1.2%) for 1 min and centrifuged for 3 min at 9000 rpm. The supernatant was then pushed through a 0.45 μm filter and subjected to a Sephacryl S-300 HR 16/30 gel filtration column (Pharmacia). The first green material eluting from the column contained unstacked PS II membranes with virtually the same components as BBYs (*18*).

Artificial Lipid Bilayers. Artificial lipid bilayers comprising a mixture of charged phospholipid and noncharged lipid were used to calibrate the phosphorylation level for AFM measurement. L-α-Phosphatidylinositol-4,5-diphosphate (PIP2) and 1,2-dioleoyl-*sn*-glycero-3-phosphocholine (DOPC, Avanti) were desolved in chloroform (1 mg/mL) and mixed at ratios of 1:100 and 1:200. The mixtures were then dropped onto the surface of freshly cleaved mica. After the chloroform was evaporated, the imaging buffer was dropped onto the samples and stayed for 1 h for bilayer formation. The samples were then gently washed twice with the buffer to remove the lipid and bilayers which were not firmly attached. The heights of the bilayers were measured by the AFM.

Thylakoid Phosphorylation. Thylakoid membranes were phosphorylated as described in Drepper et al. (*5*). For protein phosphorylation, thylakoid membranes were suspended in 50 mM Tricine−KOH (pH 7.6), 20 mM NaCl, 5 mM $MgCl_2$, and 100 mM sorbitol at a chlorophyll concentration of 0.4 mg/mL at 4 °C. Then 0.4 mM ATP and 10 mM NaF (phosphatase inhibitor) were added to the suspension which was then illuminated (500 μmol of photons m^{-2} s^{-1}) for 10 min. It is worth pointing out that Aro and co-workers found that in this high light condition, PS II core proteins have the highest levels of phosphorylation but this level of irradiance can also dephosphorylate LHC II proteins (*19*). However, in the same paper, they also demonstrate that this high light induced inactivation of LHC II phosphorylation only occurs in vivo. For isolated thylakoids, LHC II remains phosphorylated, even under these high light levels (*19*). This could indicate it might be the absence of the phosphatase which is responsible for dephosphorylating LHC II proteins in vitro.

In Situ Membrane Dephosphorylation. In situ membrane dephosphorylation was carried out by injecting 5 units of calf intestine alkaline phosphatase into 200 μL of imaging buffer containing phosphorylated membranes and 5 mM $MgCl_2$ which the phosphorylated membranes were sitting in. The membrane height was measured on mica before and after the injection.

RESULTS AND DISCUSSION

A surface-tip interaction in aqueous solution is well represented by the Derjaguin, Landau, Verwey, Overbeek (DLVO) force assuming the surface to be of infinite extent. The DLVO force (F_{DLVO}) consists of only electrostatic (F_{el}) and van der Waals (F_{vdW}) interactions, neglecting other interactions such as hydrogen forces, steric forces, and ion radii effects etc. (*15*). The force between a tip of radius R and a flat surface can be written as (*15*, *20*)

$$F_{DLVO} = F_{el}(Z) + F_{vdW}(Z) = \frac{4\pi\sigma_s\sigma_t R\lambda_D}{\epsilon_e\epsilon_0} e^{-z/\lambda_D} - \frac{H_a R}{6z^2} \quad (1)$$

where σ_s and σ_t are the charge densities of the sample surface and AFM tip, respectively, ϵ_0 is the permittivity of the free space, ϵ_e is the dielectric constant, H_a is the Hamaker constant, and z is the distance between the tip and the surface. λ_D (Debye length) indicates the exponential decrease in the potential resulting from screening the surface charges by electrolytes. λ_D is strongly dependent on the concentration and the valence of the electrolyte in the aqueous environment. For monovalent electrolytes, $\lambda_D = 0.304/\sqrt{e_c}$, where e_c is the electrolyte concentration (*20*).

The apparent height of a membrane placed on a surface is therefore a function of the relative charge densities of

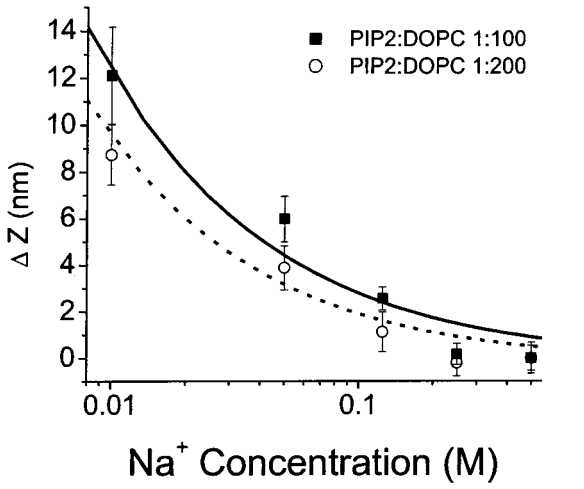

(a)

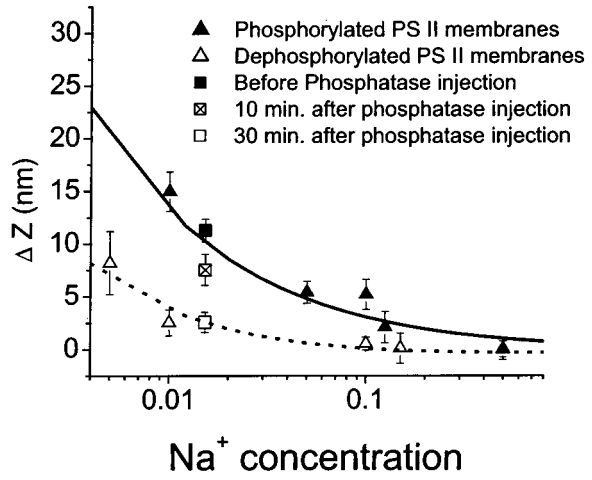

(b)

FIGURE 1: Electrostatic contribution to membrane height (ΔZ) showing data and curves fitted by DVLO theory. (a) Artificial lipid bilayers with different phosphate densities. PIP2/DOPC 1:100 bilayer (■) has an average phosphate density of 0.031 P_i/nm^2; PIP2/DOPC 1:200 bilayer (○) has an average phosphate density of 0.016 P_i/nm^2. Each point is an average of more than 60 bilayers in the field of view of the AFM. Error bars represent standard errors. The solid line shows the fitted curve for PIP2/DOPC 1:100; the dotted line shows the fitted curve for PIP2/DOPC 1:200. (b) PS II enriched membranes before and after membrane protein phosphorylation by light-activated kinase(s). The calibrated charged phosphate densities of phosphorylated (▲) and dephosphorylated (△) PS II enriched membranes are 0.0021 ± 0.0004 and 0.046 ± 0.005 P_i/nm^2, respectively. The solid line shows the fitted curve for phosphorylated PS II membranes; the dotted line shows the fitted curve for dephosphorylated PS II membranes. The effect of in situ dephosphorylation by alkaline phosphatase is also shown in this graph. Dephosphorylation was performed by injecting calf intestine alkaline phosphataes into the imaging buffer containing 5 mM $MgCl_2$. The symbols ■, x in open square, and □ show ΔZ prior to, 10 min after, and 30 min after enzyme injection. 5 mM $MgCl_2$ has a screening effect equal to 15.2 mM NaCl [λ_D for divalent 1:2 electrolyte is $0.174/\sqrt{e_c}$ (*15*)]. Each point is an average over 30 membranes in the field of view of the AFM.

membrane and surface, and the screening electrolyte (*14*). Figure 1b shows a height measurement of PS II enriched thylakoid membranes before and after phosphorylation. In this graph, the height difference between the measured membrane height and the membrane height at high electrolyte concentrations, where all long-range electrostatic forces are screened out, is labeled as ΔZ. In 500 mM Na^+, the measured heights are 12.3 ± 0.8 nm for phosphorylated PS II membranes and 10.8 ± 1.0 nm for dephosphorylated PS II membranes. In low electrolyte concentrations, it is clear from the graph that, as expected, the average measured heights of the phosphorylated membranes were higher than the nonphosphorylated ones due to the DLVO force between tip and surfaces.

Obtaining the absolute charge density of a biological membrane has proven to be problematic. For instance, the apparent charge density of purple membrane from *Halobacterium halobium* varies by a factor of 300 depending on the calibration method used (*14*). According to DLVO theory, the electrostatic contribution to membrane height (ΔZ) is given by the expression (*15*):

$$\Delta Z(e_c) = -\frac{0.304}{\sqrt{e_c}} \ln\left(\frac{F_{AFM}\epsilon_e\epsilon_0\sqrt{e_c}}{0.304 \times 4\pi R\sigma_s\sigma_t}\right) \qquad (2)$$

Apart from the electrolyte concentration and the charge density of the sample surface, the measured height is also a function of the charge density and the radius of the AFM tips. The charge density and radius of AFM tips are not certain and could vary greatly from material to material and from tip to tip. This increases the difficulty in converting a measured height to a surface charge density. Moreover, the measured height is also affected by the dielectric behind the membranes and around the tip, not just the dielectric between them as the Born energy is modulated by the electrostatic environment around the charges. Any calibration method must therefore recreate the dielectric geometry of the sample.

To minimize these problems/effects and obtain the most accurate calibration result, we used artificial lipid bilayers doped with charged lipids to mimic biological membranes as closely as possible. Known charge densities were achieved by controlling the mixture of charged, L-α-phosphatidylinositol-4,5-diphosphate (PIP2), and noncharged phospholipids, 1,2-dioleoyl-*sn*-glycero-3-phosphocholine (DOPC), to calibrate the phosphorylation level on thylakoid membranes. The average phosphate densities in bilayers of 100:1 DOPC/PIP2 and 200:1 DOPC/PIP2 are 0.031 and 0.016 P_i/nm^2 (P_i indicates the charged phosphate group), respectively, assuming the size of one lipid headgroup on the membrane is 64 Å^2. The height of these two mixed bilayers was then measured by AFM, and the experiment result was then fitted to DVLO theory. It is worth noting that the histograms of the membrane height distributions were reasonably Gaussian, but that membranes doped to a level of 50:1 DOPC/PIP2 showed marked deviations from the DLVO curve.

The experimental result and the fitted curves can be seen in Figure 1a. The electrostatic height contribution was set to zero at 0.5 M Na^+ solution. In this calibration, the same tips were used in all membrane measurements, but tips from the same batch were cross-checked and showed no measurable difference. The charge density of the tip can be estimated from Figure 1a and eq 2 as 0.256−2.088 C/m^2 provided the radius of the tip is 5−40 nm as given by the manufacturer. This uncertainty in tip charge density can be removed by our calibration since the same tips were used in all measurements, and as the same force was applied, F_{AFM} in eq 2 is a constant. ϵ_e and ϵ_0 of our lipid bilayer standards and biological membranes were assumed to be the same. The

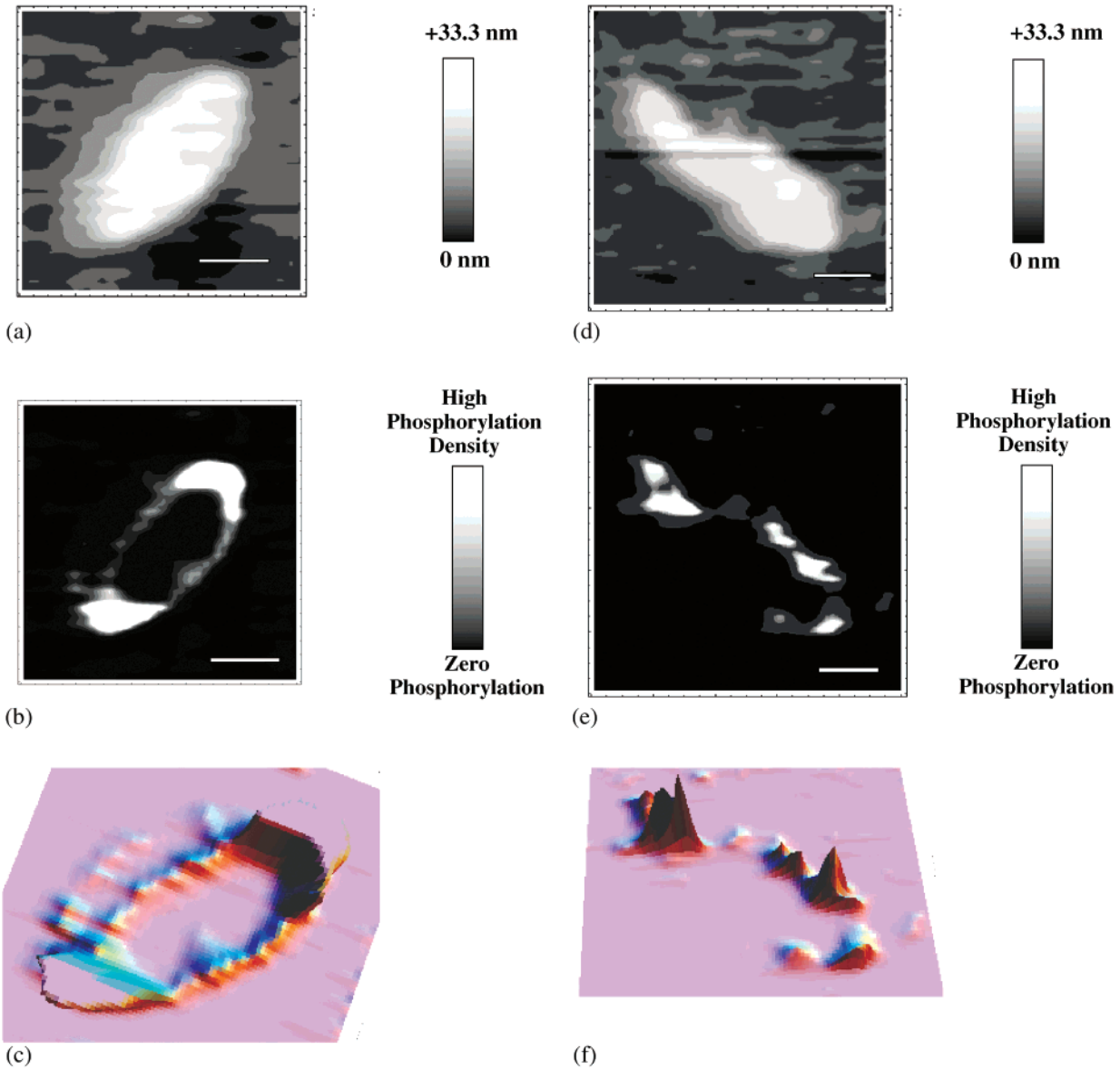

FIGURE 2: Phosphate density maps of two phosphorylated PS II membranes. Topography images (a, d), phosphate density maps (b, e), and 3D views of phosphate density maps (c, f). The charged phosphate densities were converted from the ΔZ between phosphorylated and dephosphorylated PS II membranes using DLVO theory. The dephosphorylation was performed on in situ membranes attached to mica in 10 mM Bis-Tris buffer, pH 6.5, with 5 mM $MgCl_2$. The white bars in images represent 200 nm.

electrostatic height contribution, ΔZ, then will be only a function of the charge density of the surface and the electrolyte concentration in aqueous solution. Equation 2 can therefore be rewritten as

$$\Delta Z(e_c) = -\frac{0.304}{\sqrt{e_c}} \ln\left(\frac{K\sqrt{e_c}}{\sigma_s}\right) \quad (3)$$

where

$$K = \frac{F_{AFM}\epsilon_e\epsilon_0}{0.304 \times 4\pi R\sigma_t}$$

The calibration is achieved by calculating ΔZ using DLVO theory applied to known mixtures of DOPC and PIP2. This allows K to be deduced for a particular tip, and that tip is then be used to measure ΔZ in photosynthetic membranes. The charge density of the biological membranes was calculated using calibrated tips. Phosphorylation by the membrane-bound kinases increased the charge density from 0.0021 ± 0.0004 to 0.046 ± 0.005 P_i/nm^2, in another words, 0.044 ± 0.005 phosphate group was added to every nm^2, or one phosphate per 20 nm^2 on average.

In situ dephosphorylation of phosphorylated PS II enriched membranes was also measured by the AFM (Figure 2b). The dephosphorylation was carried out by injecting calf intestine alkaline phosphatase into the sample while it was in the AFM. The dephosphorylation reaction was measured by detecting the electrostatic height contribution change using the AFM tip. After 10 min, partial removal of phosphates had occurred, with complete dephosphorylation 30 min after phosphatase injection. This demonstrates that the AFM has the capacity to monitor phosphatase and kinase kinetics in situ.

Biochemical studies of phosphorylation in chloroplasts have suggested that 65−70% of the phosphorylation is on the light-harvesting complex II (LHC II) trimers (*1*). In PS II membranes, the phosphorylatable components are the LHC

II trimer, the D1, D2 reaction center subunits, the CP43, CP29 antenna proteins, and the 10 kDa PsbH protein (*3*, *21*, *22*). There is disagreement in the literature regarding the number of phosphorylation sites on each LHC II monomer (*23*, *24*); the most accepted phosphorylation sites on these proteins are certain threonine residues (*23*, *25*) while anti-phosphotyrosine antibody studies on the thylakoids showed that the phosphorylation of tyrosine is also possible (*4*). An estimation made by Boekema et al. suggested that in ordered PS II thylakoid membrane fragments, the PS II complex containing two PS II heterodimers has a density of 1140−1190 PS II complexes/μm^2 (*17*). If we accept that 1 PS II complex associates 8 LHC II trimers (4 for each PS II reaction center) as suggested by biochemical evidence (*26*) and that only D1, D2, CP43, CP29, PsbH, and LHC II can be phosphorylated, and that each has 1 site, then there will be 34 phosphorylation sites in 1 complete PS II complex. The density of the variable phosphates will be, therefore, 40 000 $\pm$ 1000 $P_i/\mu m^2$ or 0.040 $\pm$ 0.001 P_i/nm^2. Our measurements show 0.044 $\pm$ 0.005 phosphate/nm^2, which agrees rather well with the estimation by Boekema.

As both the kinetics of the dephosphorylation and the absolute levels of charge can be measured, the final element is to create a charge map of the membrane surface. We achieved this by differencing topographic images of individual membranes before and after the action of the phosphatase. The spatial resolution in these images is limited by the relatively blunt tips used and the signal-to-noise limitations of our instrument.

Images from electrostatic difference mapping of two phosphorylated PS II enriched membranes prior to and after alkaline phosphatase injection are shown in Figure 2. These difference maps effectively show how the density of phosphorylation varies across the membranes. The most striking aspect of these images is that the phosphorylation density is significantly higher around the margin of the membranes than in the center.

In granal stacks, the periphery of the membranes is in contact with marginal regions containing PS I, and our results suggest some functional differentiation within the PS II rich region at the center of the grana. As the initial phosphorylation is performed in vitro, we cannot tell whether this distribution is a result of protein redistribution following phosphorylation, or whether it reflects functional differentiation prior to phosphorylation.

DVLO theory is a mean field theory, in this case representing the interaction between a spherical tip and an infinite surface. While this is suitable for low-resolution average measurements of the height of reasonably large membrane patches, it is unlikely to provide a good representation of charge densities for smaller objects/regions. The charge density maps of Figure 2 are linearized to be proportional to charge densities assuming that DLVO theory holds. This is unlikely to be accurate for small features. In fact, one of these plots peaks at 17 phosphates/nm^2, an impossible value which probably reflects the need for interpretation of the data via a theory other than a mean field one.

We estimate that the spatial resolution of these images is approximately 50 nm. It should be possible to improve this significantly even using conventional AFM tips. We predict that electrostatic difference mapping using appropriate tips and an appropriate AFM has both the sensitivity and spatial resolution to allow individual phosphorylation sites to be located with a spatial resolution of 10 nm or better. Future work will determine whether this is indeed possible or not.

CONCLUSIONS

- It is possible to create a phosphorylation difference map of membranes with a resolution better than 100 nm.
- The average phosphorylation level in PS II enriched granal stacks is 0.044 $\pm$ 0.005 phosphate/nm^2.
- Phosphorylation in higher plant grana is concentrated at the margins.

ACKNOWLEDGMENT

We thank Professor Richard Templer for discussions regarding lipid bilayer deposition on mica, and Dr. Rudiger Woscholski for stimulating discussions regarding the PIP2 calibration method and for providing the PIP2 and phosphatase.

REFERENCES

1. Larsson, U. K., Jergil, B., and Andersson, B. (1983) *Eur. J. Biochem. 136*, 25−29.
2. Kyle, D. J., Staehelin, L. A., and Arntzen, C. J. (1983) *Arch. Biochem. Biophys. 222*, 527−541.
3. Kruse, O., Zheleva, D., and Barber, J. (1997) *FEBS Lett. 408*, 276−280.
4. Tullberg, A., Håkansson, G., and Race, H. L. (1998) *Biochem. Biophys. Res. Commun. 250*, 617−622.
5. Drepper, F., Carlberg, I., Andersson, B., and Haehnel, W. (1993) *Biochemistry 32*, 11915−11922.
6. Coughlan, S. J., and Hind, G. (1986) *J. Biol. Chem. 261*, 14062−14068.
7. Coughlan, S. J., and Hind, G. (1986) *J. Biol. Chem. 261*, 11378−11385.
8. Gal, A., Herrmann, R. G., Lottspeich, F., and Ohad, I. (1992) *FEBS Lett. 298*, 33−35.
9. Race, H. L., and Hind, G. (1996) *Biochemistry 35*, 13006−13010.
10. Sokolenko, A., Fulgosi, H., Gal, A., Altschmid, L., Ohad, I., and Hermann, R. G. (1995) *FEBS Lett. 371*, 176−180.
11. Binnig, G., Quate, C. F., and Gerber, C. (1986) *Phys. Rev. Lett. 56*, 930−933.
12. Butt, H.-J. (1991) *Biophys. J. 60*, 1438−1444.
13. Butt, H.-J. (1991) *Biophys. J. 60*, 777−785.
14. Butt, H.-J. (1992) *Biophys. J. 63*, 578−582.
15. Müller, D. J., and Engel, A. (1997) *Biophys. J. 73*, 1633−1644.
16. Berthold, D. A., Babcock, G. T., and Yocum, C. F. (1981) *FEBS Lett. 134*, 231−234.
17. Boekema, E. J., van Breemen, J. F. L., van Roon, H., and Dekker, J. P. (2000) *J. Mol. Biol. 301*, 1123−1133.
18. van Roon, H., van Breemen, J. F. L., de Weerd, F. L., Dekker, J. P., and Boekema, E. J. (2000) *Photosynth. Res. 64*, 155−166.
19. Rintamäki, E., Salonen, M., Suoranta, U.-M., Carlberg, I., Andersson, B., and Aro, E.-M. (1997) *J. Biol. Chem. 272*, 30476−30482.
20. Israelachvili, J. (1991) *Intermolecular & surface forces*, 2nd ed., Academic Press Ltd., London, U.K.
21. Testi, M. G., Croce, R., Laureto, P. P., and Bassi, R. (1996) *FEBS Lett. 399*, 245−250.
22. Silverstein, T., Cheng, L., and Allen, J. F. (1993) *FEBS Lett. 334*, 101−105.
23. Pursiheimo, S., Rintamäki, E., Baena-Gonzales, E., and Aro, E.-M. (1998) *FEBS Lett. 423*, 178−182.
24. Dilly-Hartwig, H., Allen, J. F., Paulsen, H., and Race, H. L. (1998) *FEBS Lett. 435*, 101−104.
25. Nilsson, A., Stys, D., Drakenberg, T., Spangfort, M. D., Forsén, S., and Allen, J. F. (1997) *J. Biol. Chem. 272*, 18350−18357.
26. Peter, G. F., and Thornber, J. P. (1991) *J. Biol. Chem. 266*, 16745−16754.

BI025962S